SCIENTIFIC REPORTS

OPEN

SUBJECT AREAS:
PHYSICAL CHEMISTRY
SURFACE CHEMISTRY
MEMBRANE BIOPHYSICS
MEMBRANE STRUCTURE AND ASSEMBLY

Received
4 February 2013

Accepted
30 April 2013

Published
16 May 2013

Correspondence and requests for materials should be addressed to Z.C. (zhanc@umich.edu)

Physiologically-Relevant Modes of Membrane Interactions by the Human Antimicrobial Peptide, LL-37, Revealed by SFG Experiments

Bei Ding[1], Lauren Soblosky[1], Khoi Nguyen[1], Junqing Geng[1,2], Xinglong Yu[2], Ayyalusamy Ramamoorthy[1,3] & Zhan Chen[1,3]

[1]Department of Chemistry, University of Michigan, Ann Arbor, MI 48109, [2]Department of Precision Instrument, Tsinghua University, Beijing, 100084, China, [3]Biophysics, University of Michigan, Ann Arbor, MI 48109.

Antimicrobial peptides (AMPs) could become the next generation antibiotic compounds which can overcome bacterial resistance by disrupting cell membranes and it is essential to determine the factors underlying its mechanism of action. Although high-resolution NMR and other biological studies have provided valuable insights, it has been a major challenge to follow the AMP-membrane interactions at physiologically-relevant low peptide concentrations. In this study, we demonstrate a novel approach to overcome this major limitation by performing Sum Frequency Generation (SFG) vibrational spectroscopic experiments on lipid bilayers containing an AMP, LL-37. Our results demonstrate the power of SFG to study non-linear helical peptides and also infer that lipid-peptide interaction and the peptide orientation depend on the lipid membrane composition. The observed SFG signal changes capture the aggregating process of LL-37 on membrane. In addition, our SFG results on cholesterol-containing lipid bilayers indicate the inhibition effect of cholesterol on peptide-induced membrane permeation process.

The development of drug resistance by many bacteria against traditional antibiotics poses an important challenge in curing infectious disease. Extensive research has been performed to develop antimicrobial peptides into powerful antibiotics to kill bacteria[1–7]. Because most antimicrobial peptides disrupt the cell membranes of bacteria, it is difficult for bacteria to develop drug resistance against antimicrobial peptides. However, the detailed interaction mechanisms between many antimicrobial peptides and bacterial cell membranes remain unclear.

LL-37, the only cathelicidin member in humans, plays an important role in human innate immunity system[8,9]. LL-37 exhibits a broad-spectrum antimicrobial activity and lipopolysaccharide-neutralizing effects. There is considerable therapeutic interest in utilizing LL-37 to overcome the bacterial resistance against traditional antibiotics and therefore there is significant interest in understanding its mechanism of action. Studies have reported the biological effects of LL-37 as well as the interactions of LL-37 with various types of lipid membranes. It was found that LL-37 readily disrupts the negative charged 1,2-dipalmitoyl-sn-glycero-3-phospho-(1′-rac-glycerol) (sodium salt) (DPPG) monolayer but exerts no effect on neutral charged 1,2-dipalmitoyl-sn-glycero-3-phosphocholine (DPPC) and 1,2-dipalmitoyl-sn-glycero-3-phosphoethanolamine (DPPE) monolayers by specular X-ray reflectivity[10]. NMR techniques have been used to determine 3D structures of LL-37 associated with neutral n-dodecylphosphocholine (DPC)[11] and negative-charged sodium dodecyl sulfate (SDS) micelles[12]. Although the peptide structures are not completely the same in these two environments, they both feature a kink in the middle of the peptide. Solid-state NMR studies revealed the oligomerization[13], membrane orientation and carpet mechanism action for the peptide[14]. While solid-state NMR and calorimetric studies have provided insights into the mechanism of action for LL-37, obtaining such information at very low, physiologically relevant concentrations have been a major limitation. Methods to overcome this limitation not only can be used to study other AMPs but also other membrane active peptides/proteins including cell penetrating peptides and amyloid proteins.

In this study, we demonstrate the power of the sum frequency generation (SFG) vibrational spectroscopic technique to study the interactions between LL-37 and a single lipid bilayer containing different ratios

of negative-charged 1-palmitoyl-2-oleoyl-sn-glycero-3-phosphoglycerol (POPG), neutral-charged 1-palmitoyl-2-oleoyl-sn-glycero-3-phosphocholine (POPC), and cholesterol for various peptide concentrations. SFG spectroscopy is an intrinsic surface-sensitive technique[15–22] and has been widely used to study the structure and orientation of peptides and proteins at bio-interfaces[23–27]. Because of the excellent sensitivity, SFG can be used to investigate peptide-membrane interactions in the physiologically-relevant peptide concentration range, which cannot be done using most other biophysical techniques[28–31].

Most of the previous orientation studies on α-helical peptides using SFG were focused on the linear α-helical structure[32,33]. For peptides that are not linear, data analysis on linear peptides was still used to determine orientation[34]. Here, we studied a non-linear α-helical structure using SFG and developed approaches to analyze the data for the first time in the literature. We considered two types of non-linear α-helical structure in this study: a bent structure and a disrupted structure. The bent structure changes in the helix axis direction with all the residues remaining helical, an example of which is LL-37 associated with SDS vesicles[12]. The disrupted structure also bears a change in the axial direction but with a loss of the helical character of the residues around the kink location, such as melittin, alamethicin and LL-37 associated with DPC vesicles[11]. For both "bend and disruption" models, we treat the helical part as two adjacent segments. The way we treat the first segment is the same as for an ideal linear helix previously reported[32,33], but the calculation for the second segment is different for two models. For the bend model, since there is no random structure between the two segments, we ought to consider that the entire helical LL-37 structure is continuous. Especially, there is a phase term involved in the calculation of the E1 vibrational mode which should also be continuous for the entire LL-37 helical structure. On the contrary, the phases for the vibrations of the two segments in the disrupted structure are unrelated and we do not consider the phase continuation. More calculation details (i.e. the values for the dipole moments and the Raman tensors) are included in the supporting information. The peptide membrane orientation deduced using SFG is compared to results from NMR studies. Our results demonstrate that at the high peptide concentrations, SFG results are compatible to the NMR data. Different from NMR, SFG has the capability to investigate very low concentrations of complex α-helical structures and their membrane orientations.

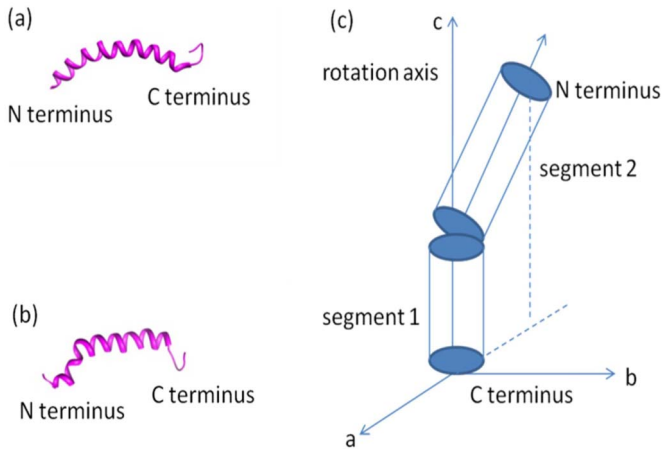

Figure 1 | Structures of LL-37 (a) associated with SDS vesicles[12] (PDB: 2K6O) (b) associated with DPC vesicles[11] (PDB: reported by Ramamoorthy group) (c) A cartoon representation of the LL-37 molecular structure and the rotation axis.

Results

Structures of LL-37 in SDS[12] and DPC[11] micelles were reported based on solution NMR studies (Figure 1). The continuous helical region includes the residues 2–31 in SDS with a bend between residues 14–16. The bend is caused by the hydrophobic interaction between residues Ile13 and Phe17 and the membrane. The angle between the two helical segments connected by the bend is about 143° (Figure 1a). We developed the "bend model" to determine the peptide orientation in POPG lipid bilayers for our SFG study. The structure of LL-37 associated with zwitterionic DPC micelles was also reported based on a solution NMR study[11]. The well-structured region is from residues 4 to 33 and the helix-break-helix motif was highlighted with a break at residue Lys-12 (Figure 1b). Both structural studies suggest a tight cluster formed by residue Ile13 and Phe17. In contrast to the LL-37 structure in SDS vesicles, where the N-terminal region is rigid, the N terminus of LL-37 was found to be dynamic in DPC micelles. Since there is a disruption in LL-37 helicity when associated with zwitterionic lipid vesicles, we adopt the "disruption model" to address the disruption in the LL-37 helical structure for SFG data analysis. Since the N terminus is dynamic, we calculated the orientation dependence of the nonlinear optical susceptibility components for structures with different residue numbers in the N terminal α-helical region to ensure that our model is reliable (Figure 2). A schematic of the

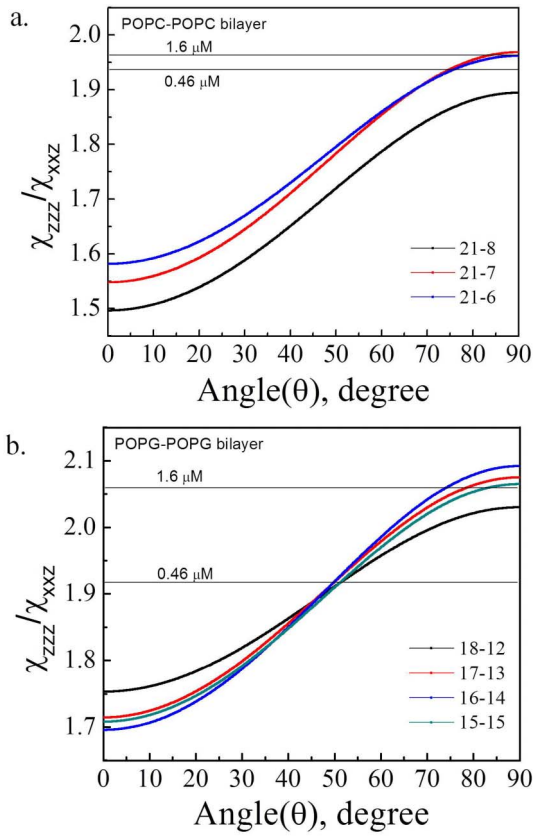

Figure 2 | (a) Dependence of the calculated SFG $\chi^{(2)}_{zzz}/\chi^{(2)}_{xxz}$ ratio of LL-37 associated with a POPC/POPC bilayer on the helix tilt angle (first segment) relative to the bilayer surface normal. The first segment has 21 amino acid residues, and the second segment has 6, 7, and 8 amino acid residues respectively (the disruption model). (b) Dependence of the calculated SFG $\chi^{(2)}_{zzz}/\chi^{(2)}_{xxz}$ ratio of LL-37 associated with a POPG/POPG bilayer on the helix tilt angle (first segment) relative to the surface normal. 18–12, 17–13, 16–14, and 15–15 refer to the peptides with the first α-helical segment of 18, 17, 16, and 15 amino acid residues and the second α-helical segment of 12, 13, 14, and 15 amino acid residues respectively (the bend model).

LL-37 molecule and the molecular axes used for SFG data analysis is shown in Figure 1c.

Since LL-37 has a random coil structure for the N-terminal residues, we need to ensure that the detected SFG amide I signal is dominated by the contributions from the α-helical component. Contribution to the entire SFG signal from the unstructured region of the peptide was calculated by NLOPredict developed by the Simpson group[35] for both the bent and disrupted structures of LL-37. We found that for both the membrane-surface and transmembrane orientations, the SFG signal contribution from random coil structured regions is less than 5% of the total SFG signal (supporting information, even under the assumption that the peak of the random coil overlaps with that of the α-helical components). Therefore, it is reasonable to assume that the signal attributed to the α-helical structured region of the peptide is the main contributor to the measured SFG signal in the amide I region.

SFG spectra collected with ssp and ppp polarization combinations from LL-37 associated with POPC/POPC bilayers in the amide I frequency region at 0.46 μM and 1.6 μM concentrations are shown in Figure 3a. Here, for the SFG signals in the amide I frequency range, we collected spectra using two polarization combinations, ssp and ppp, in order to deduce the LL-37 orientation from the spectral fitting result $\chi_{eff,ppp}/\chi_{eff,ssp}$. The SFG spectra in Figure 3a exhibit a single peak centered around ~1647 cm^{-1}, indicating an α-helical structure. The SFG spectral intensities for the two studied concentrations are very similar, and the fitting results of $\chi_{eff,ppp}$ and $\chi_{eff,ssp}$ are displayed in Table 1a. Using the spectral fitting results and the "disruption model" (Figure 2a), the orientation analysis shows that the LL-37 peptide lies more or less parallel to the membrane surface with a tilt angle between 56° and 90° relative to the lipid bilayer normal at the peptide concentration of 0.46 μM and 68° to 90° at the peptide concentration of 1.6 μM. The similar orientation and SFG spectral intensities indicate that the adsorption amounts of LL-37 at 0.46 μM and 1.6 μM are similar.

SFG signals detected in the frequency range of 3000–3600 cm^{-1} before and after the addition of LL-37 to the POPC/POPC bilayer subphase are shown in Figure 3b. Since the POPC headgroup is neutral, the POPC/POPC bilayer associated water molecules do not have a preferred orientation, therefore no water O-H stretching SFG signal was detected prior to the addition of the LL-37 stock solution into the subphase. After the addition of LL-37, a broad SFG signal in this frequency range was detected, which is mostly attributed to the water O-H stretching mode and the N-H stretching peak (centered at 3280 cm^{-1}) of LL-37. Because LL-37 is positively charged, the ordered LL-37 molecules associated with the POPC/POPC bilayers can induce ordering of surrounding water molecules

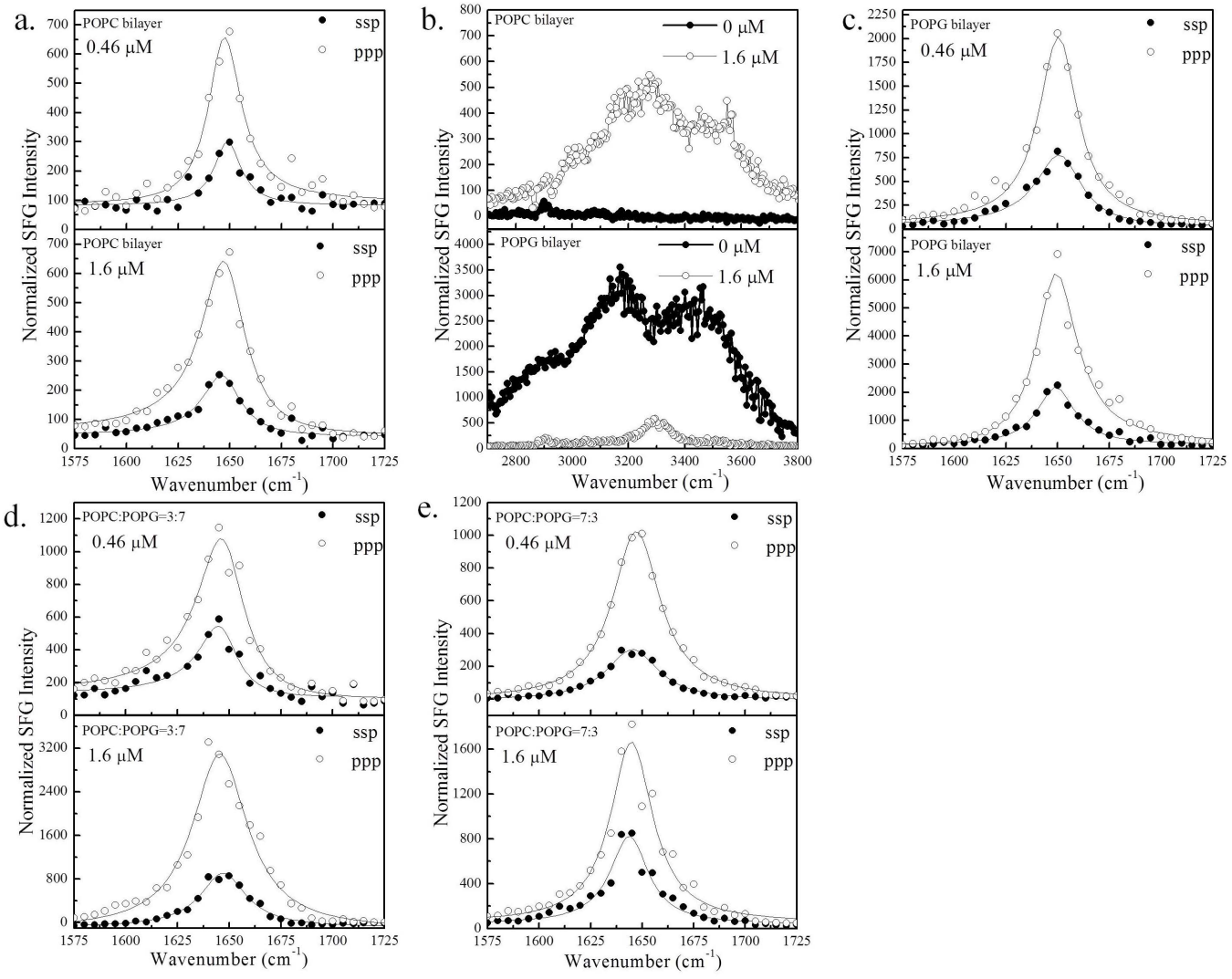

Figure 3 | (a) SFG amide I spectra of LL-37 associated with POPC/POPC bilayer; (b) SFG O-H/N-H stretching signals collected from the POPC (top) and POPG (bottom) bilayers in contact with LL-37 solution (1.6 μM); SFG amide I spectra of LL-37 associated with (c) POPG/POPG bilayer, (d) 3 : 7 POPC:POPG and (e) 7 : 3 POPC:POPG lipid bilayers.

Table 1 | Fitting parameters of the SFG amide I spectra of LL-37 associated with (a) POPC/POPC, (b) POPG/POPG, (c) POPC:POPG = 7 : 3, and (d) POPC:POPG = 3 : 7 bilayers

(a)

POPC/POPC	Polarization	Peak center (cm^{-1})	Peak Width (cm^{-1})	χ_{eff}	Ratio	Tilt angle	Adsorption amount
0.46 μM	ssp	1649	7.9	14.8	1.94 ± 0.13	56–90	1.1
	ppp	1647	9.7	23.7			
1.6 μM	ssp	1649	13.5	14.3	1.96 ± 0.06	68–90	1.1
	ppp	1647	11.3	24.2			

(b)

POPG/POPG	Polarization	Peak center (cm^{-1})	Peak Width (cm^{-1})	χ_{eff}	Ratio	Tilt angle	Adsorption amount
0.46 μM	ssp	1648	13	33.6	1.92 ± 0.04	44–58	1.0
	ppp	1650	12	56.5			
1.6 μM	ssp	1649	11	45.3	2.06 ± 0.07	62–90	2.8
	ppp	1649	12	78.3			

(c)

POPC:POPG = 7 : 3	Polarization	Peak center (cm^{-1})	Peak Width (cm^{-1})	χ_{eff}	Ratio	Tilt angle
0.46 μM	ssp	1645	13.8	17.11	2.02 ± 0.01	63–80
	ppp	1648	13.7	30.6		
1.6 μM	ssp	1646	11.2	26.9	1.68 ± 0.07	0–15
	ppp	1649	13.9	42.1		

(d)

POPC:POPG = 3 : 7	Polarization	Peak center (cm^{-1})	Peak Width (cm^{-1})	χ_{eff}	Ratio	Tilt angle
0.46 μM	ssp	1648	14.0	20.3	1.72 ± 0.01	0–15
	ppp	1646	11.5	30.8		
1.6 μM	ssp	1651	13.8	28.0	2.07 ± 0.05	65–90
	ppp	1651	10.6	51.6		

that generate the SFG O-H stretching signal. Since the POPC/POPC bilayer is neutral, the observed SFG signal in this range suggests that LL-37 potentially interacts with the POPC/POPC bilayer by hydrophobic interaction instead of electrostatic interaction.

The membrane surface orientation of LL-37 associated with the POPC bilayer deduced by the SFG amide I signal in this study is in excellent agreement with solid-state NMR results[8,14].

The amide I signals observed for LL-37 associated with POPG/POPG lipid bilayers (Figure 3c) feature a single peak at ~1649 cm^{-1}, similar to the POPC/POPC case. The SFG intensities for the high and low peptide concentrations are similar in both polarization combinations in a POPC/POPC system. However, there is a significant increase in the SFG intensity when the concentration is increased in the POPG/POPG system. The spectra were fitted with parameters displayed in Table 1b and the ratios of $\chi_{eff,ppp}$ and $\chi_{eff,ssp}$ were used to deduce the orientation angles. Since previous NMR studies indicated that LL-37 has a bend in the middle when associated with negatively charged vesicles, we adopt the "bend model" discussed above to examine LL-37's orientation associated with POPG/POPG lipid bilayers (Figure 2b). This model considers the phase continuity between the vibrational modes of the two segments in the data analysis; details can be found in the supporting information. Our analysis shows that LL-37 orients with a tilt angle of 44° to 58° relative to the POPG/POPG surface normal for the 0.46 μM peptide concentration case and 62° to 90° for the 1.6 μM concentration case. These results reveal that the membrane orientation of LL-37 in POPG/POPG bilayer is dependent on the peptide concentration and, at low concentrations, the peptides tilt to form a transmembrane orientation. This change in the peptide orientation could be attributed to the oligomerization of the peptide as observed from solid-state NMR experiments[13].

SFG signals collected in the frequency range of 3000–3600 cm^{-1} before and after the addition of LL-37 (with the final concentration of 1.6 μM) to the POPG/POPG bilayer subphase are shown in Figure 3b. Before the addition of the LL-37, the spectra showed two broad peaks at ~3200 cm^{-1} and ~3500 cm^{-1} which can be explained as follows: the negatively charged lipid headgroups of the POPG/POPG bilayer facilitate the ordering of the associated water molecules, resulting in prominent water O-H stretching SFG signals. However, after LL-37 was added to the subphase, the two broad peaks diminished and a new peak centered at 3300 cm^{-1} appeared (Figure 3b). With LL-37 added, we expect the cationic peptide molecules associated with the negatively-charged POPG/POPG bilayer partially neutralized the bilayer charge. The originally ordered water molecules induced by the charged lipids would be less ordered, leading to a substantial decrease or even disappearance of the SFG water signal as shown in Figure 3b. The new 3300 cm^{-1} is likely from the N-H stretching mode of the peptide molecules due to the existence of ordered LL-37 molecules on the membrane surface.

In order to better simulate the real cell membrane which contains mixed lipids, we also investigated LL-37 interacting with mixed lipid bilayers with different negatively charged and zwitterionic lipid ratios. For a POPC:POPG = 3 : 7 bilayer, the interaction result with LL-37 has a similar trend as that with the pure POPG system (Figure 3d). After increasing the LL-37 peptide concentration from 0.46 μM to 1.6 μM, the peptide orientation changed from perpendicular to the membrane surface (0~15° vs. the surface normal) to parallel to the surface (70~90° vs. the surface normal) if we assume the peptide adopts the same structure as in negative charged SDS vesicles. This shows that when LL-37 interacts with the mixed bilayer, LL-37 molecules target the POPG component. The peptides inserted into the bilayer at low concentrations and previous research

has shown that LL-37 has a tendency to oligomerize[8]. It is likely the inserted peptides can be pulled out from the bilayer by other peptide molecules at a higher peptide concentration via hydrophobic-hydrophobic interaction.

For a POPC:POPG = 7 : 3 lipid bilayer, the orientation information deduced is somewhat complicated (Figure 3e). When the peptide concentration is 0.46 μM, the peptide molecules show a parallel orientation to the surface (65∼75° relative to the bilayer normal) if we assume that the peptide adopts the same structure as in the neutral charged DPC vesicles. Interestingly, at 1.6 μM peptide concentration, the peptide molecules have a transmembrane orientation (0∼15° relative to the bilayer normal). After increasing the peptide concentration to 4.8 μM, 6.4 μM and 7.9 μM, the peptide molecules resumed the parallel orientation, nearly lying down on the bilayer surface.

We further investigated interactions between LL-37 and two lipid bilayers containing cholesterol (CHO). 1 : 1 POPC:CHO lipid bilayer was used and we monitored the SFG signal in the amide I and O-H stretching frequency regions in the same way as in the above studies without cholesterol. The experimental results showed that after adding LL-37 peptides to the subphase, the SFG water signal increases (Figure 4a), but it is not as substantial as that observed from the pure POPC lipid bilayer system (Figure 3b). The SFG water signal is induced by the positive charge of the adsorbed LL-37 molecules and therefore it is reasonable to believe it is related to the amount of adsorbed LL-37 molecules regardless of the ordering of these LL-37 molecules. With the presence of cholesterol in the lipid bilayer, fewer LL-37 molecules interact with the lipid bilayer. In addition to the much weaker water signal, there is a striking difference in the spectral feature since there is no 3300 cm^{-1} peak in the cholesterol-containing system. No amide I signal was detected in ssp or ppp spectrum (Figure 4b). Although we believe that the POPC/CHO system has fewer LL37 molecules adsorbed, we could not assess the ordering of the adsorbed LL-37 molecules due to the low SFG amide I signal we detected.

We also investigated the incorporation of cholesterol into a lipid bilayer containing an anionic lipid: POPG:POPC:CHO = 0.3 : 0.7 : 1. After the injection of the LL-37 peptide solution into the subphase, neither discernible SFG N-H stretching signal (Figure 4a) nor SFG amide I ssp signal (Figure 4b) was detected. However, a small ppp SFG signal for the amide I band was observed. Compared to the 1 : 1 POPC:CHO lipid bilayer, this shows that the addition of negatively charged POPG to the lipid bilayer increases the surface coverage of associated LL-37 peptides. Still, the LL-37 surface coverage is significantly lower than that of LL-37 associated with the 3 : 7 POPG:POPC bilayer without CHO, suggesting that cholesterol suppresses the interaction of LL-37 with lipid bilayers. These results are in excellent agreement with solid-state NMR studies[14,36].

Discussion

We compared the relative adsorption amounts of LL-37 molecules on POPC and POPG bilayers according to the observed SFG signal intensities, as summarized in Table 1. The number of adsorbed molecules is proportional to χ_{xxz}/β_{aac}, where χ_{xxz} is deduced from the experimental SFG ssp spectrum (related to signal intensity) and β_{aac} is the microscopic hyperpolarizability component of the amide I signal of LL-37. The details of calculating the relative adsorption amounts can be found in the supporting information. The amount of LL-37 adsorption on the POPG bilayer is comparable to that on the POPC bilayer at 0.46 μM but it is ∼2.6 times larger compared to that on the POPC bilayer at 1.6 μM (supporting information). The adsorption amount of LL-37 interacting with POPG/POPG increased as the peptide concentration was raised, which can be attributed to the electrostatic interaction between the anionic lipid and the cationic peptide. The different adsorption amounts of LL-37 on POPG and POPC lipid bilayers were confirmed by surface plasmon resonance (SPR) experi-

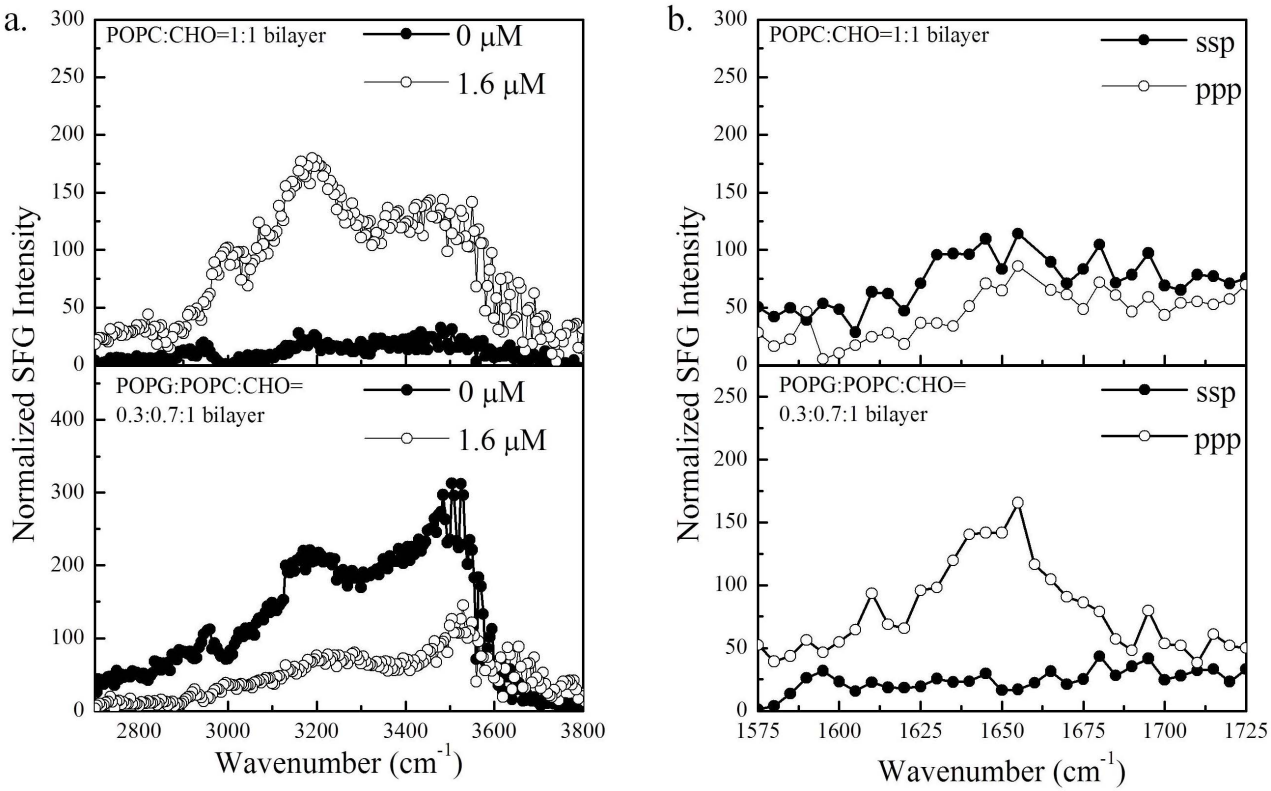

Figure 4 | (a) SFG O-H/N-H stretching signals collected from the 1 : 1 POPC:CHO (top) and 0.3 : 0.7 : 1 POPG:POPC:CHO (bottom) bilayers in contact with LL-37 solution (1.6 μM); (b) SFG amide I spectra of LL-37 associated with 1 : 1 POPC:CHO (top) and 0.3 : 0.7 : 1 POPG:POPC:CHO (bottom) bilayers in contact with LL-37 solution (1.6 μM).

ments (Figure 5). It was shown by SPR that at the concentration of 1.6 μM, the initial adsorption amount of LL-37 on POPG is ~3 times larger than that on POPC. Also, the peptides experience a certain degree of desorption on POPC but the adsorption amount remains stable on POPG. This indicates a weaker interaction between LL-37 and POPC compared to POPG. Since POPC is neutral, LL-37 only interacts with POPC via hydrophobic interactions. However, POPG is negatively charged and electrostatic interactions between the positively charged peptides and the membrane induce more peptide adsorption when the peptide concentration increases.

The differences in the membrane orientation of LL-37 on POPC and POPG lipid bilayers facilitate the understanding of its membrane interaction mode. It was reported that lipid headgroup perturbation induced by LL-37 is larger in bilayers containing a negatively charged lipid (DMPG:DMPC = 4 : 1) than in the zwitterionic DMPC bilayer, but the LL-37 molecules adopt the same parallel orientation when associated with the lipid bilayers deduced using NMR spectroscopy[37]. It was proposed that LL-37 exhibits a non-pore formation carpet mode on zwitterionic DPC vesicles[11]. Our results for LL-37 associated with the POPC/POPC and POPG/POPG lipid bilayers with a high peptide concentration of 1.6 μM supports the above conclusions: for both cases, the peptides adopt an approximately parallel orientation. As we discussed above, the unique advantage of SFG study is that SFG can be used to study the interactions between LL-37 and model cell membranes at much lower (physiologically relevant) peptide concentrations. At a lower peptide concentration of 0.46 μM, SFG results indicate that the LL-37 molecules associated with the POPG/POPG bilayer tilted towards the membrane normal. Previous LL-37 research revealed that at ~0.5 and 1.5 μM, LL-37 molecules have both monomer and dimer forms in aqueous solution[38]. Trimers were detected when peptide concentration is increased to 50 μM. At our experimental condition, i.e. 0.46 μM and 1.6 μM, which is similar to 0.5 and 1.5 μM, it is most likely that LL-37 dissolves in water as monomers or/and dimers. We believe that for the POPC/POPC bilayer, the peptide molecules saturated at a low concentration of 0.46 μM as monomers/dimers and remain so at a higher peptide concentration of 1.6 μM. However, for the POPG/POPG bilayer, the peptides penetrate into the membrane at a low concentration. While at a higher peptide concentration, the domination of the peptide-peptide interaction could drag the initially inserted peptide molecules out of the membrane, which not only changes the overall membrane orientation of the peptides, but also induces the increase of the peptide adsorption amount.

For the systems with mixed lipids, we believe that the concentration-dependent behavior can be explained as follows: Initially, at a low peptide concentration, most of the LL-37 molecules interact with the POPC lipid, which is the major component of the POPC:POPG = 7 : 3 bilayer. Therefore, the overall orientation of LL-37 is similar to that for the associated LL-37 with a pure POPC bilayer. At a slightly higher peptide concentration, more peptides can interact with the POPG lipids, which is the minor component in the bilayer. In this case, the interaction between LL-37 with the POPC:POPG = 7 : 3 bilayer is similar to the situation when a pure POPG bilayer interacts with a lower concentration of LL-37 in which LL-37 can insert into the bilayer. At higher peptide concentrations, additional peptides that associated with the bilayer pulled the inserted LL-37 out of the membrane, as in the pure POPG bilayer case which leads to a parallel orientation.

In summary, we have examined the molecular interaction of the LL-37 peptide with a variety of lipid bilayers using SFG (Figure 6), and have developed a SFG orientation analysis methodology for bent and disrupted α-helices. We have demonstrated that SFG is sensitive enough to study peptide-lipid molecular interaction at low-peptide concentrations, which is beyond other techniques such as NMR. LL-37 is shown to saturate the pure POPC lipid bilayer at a low concentration (0.46 μM) with an orientation parallel to the membrane surface. However, in pure POPG or POPC/POPG mixed lipid bilayers, LL-37 exhibits a reorientation upon changing the peptide concentration, suggesting the peptide aggregation process. In cholesterol-containing systems, SFG results demonstrate that cholesterol has a significant suppression effect on the peptide-membrane interaction. We strongly believe that the experimental and data analysis approaches developed in this study would be highly applicable in studying other membrane active systems including other AMPs, cell penetrating peptides, fusion peptides and amyloid proteins.

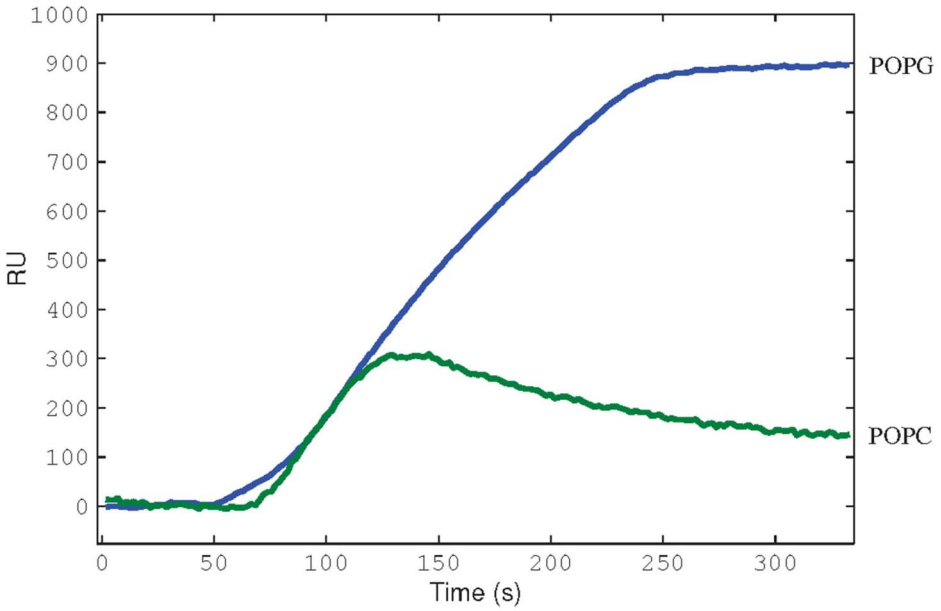

Figure 5 | Time-dependent SPR signals observed before and after LL-37 peptide solutions with 1.6 μM concentration in water were injected at 50 μl/min into the flow chambers to interact with the POPG (blue) and POPC (green) bilayers. For the POPG bilayer, the adsorption curve will reach a plateau at around 220 s. While for the POPC bilayer, peptides start to desorb from the lipid bilayer after 150 s, indicating a weaker interaction between LL-37 and the POPC bilayer compared to that with the POPG lipid bilayer.

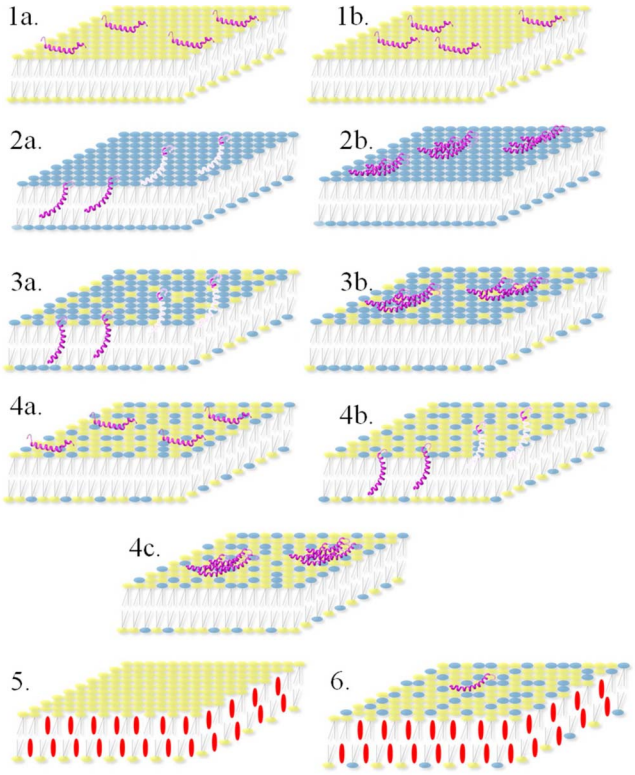

Figure 6 | Schematics showing interactions between LL-37 and different lipid bilayers. (1) POPC bilayer at a low concentration (left, 1a) and a high concentration (right, 1b); (2) POPG bilayer at a low concentration (left, 2a) and a high concentration (right, 2b); (3) 3 : 7 POPC:POPG lipid bilayer at a low concentration (left, 3a) and a high concentration (right, 3b); (4) 7 : 3 POPC:POPG lipid bilayer at a low concentration (left, 4a) and a high concentration (right, 4b) and even higher concentrations (bottom, 4c); (5) 1 : 1 POPC:CHO lipid bilayer at a high concentration; (6) 0.3 : 0.7 : 1 POPG:POPC:CHO lipid bilayer at a high concentration.

Methods

Detailed calculation and experimental details can be found in the supporting information. For most lipid bilayer systems studied in this study, two final LL-37 peptide concentrations of 0.46 μM and 1.6 μM were used. The SFG spectra were collected with ssp and ppp polarization combinations after adding the LL-37 stock solution into the subphase of the model cell membrane bilayer for 1.5 hours. The SFG signal intensity remained unchanged for the next two hours, suggesting that the equilibration of the peptide-lipid bilayer interaction was reached. All the SFG spectra exhibited a single peak at ~1650 cm^{-1} (Figure 3). The spectral fitting results as well as the ratios of χ_{zzz}/χ_{xxz} deduced from the ppp and ssp SFG spectra after deconvoluting the Fresnel factors are shown in Table 1.

1. Zasloff, M. Antimicrobial peptides of multicellular organisms. *Nature.* **415**, 389–395 (2002).
2. Ding, J. L. & Ho, B. Antimicrobial peptides: Resistant-proof antibiotics of the new millennium. *Drug Dev. Res.* **62**, 317–335 (2004).
3. Matsuzaki, K. Why and how are peptide-lipid interactions utilized for self-defense? Magainins and tachyplesins as archetypes. *Biochim. Biophys. Acta.* **1462**, 1–10 (1999).
4. Hancock, R. E. & Diamond, G. The role of cationic antimicrobial peptides in innate host defenses. *Trends Microbiol.* **8**, 402–410 (2000).
5. Epand, R. M. & Vogel, H. J. Diversity of antimicrobial peptides and their mechanisms of action. *Biochim. Biophys. Acta.* **1462**, 11–28 (1999).
6. Sitaram, N. & Nagaraj, R. Interacion of antimicrobial peptides with biological and model membranes: structural and charge requirements for activity. *Biochim. Biophys. Acta.* **1462**, 29–54 (1999).
7. Brogden, K. A. Antimicrobial peptides: pore formers or metabolic inhibitors in bacteria? *Nat. Rev. Microbiol.* **3**, 238–250 (2005).
8. Dürr, U. H. N., Sudheendra, U. S. & Ramamoorthy, A. LL-37, the only human member of the cathelicidin family of antimicrobial peptides. *Biochim. Biophys. Acta.* **1758**, 1408–1425 (2006).
9. Burton, M. F. & Steel, P. G. The chemistry and biology of LL-37. *Nat. Prot. Rep.* **26**, 1572–1584 (2009).
10. Neville, F. *et al.* Lipid Headgroup Discrimination by Antimicrobial Peptide LL-37: Insight into Mechanism of Action. *Biophys. J.* **90**, 1275–1287 (2006).
11. Porcelli, F., Verardi, R., Shi, L., Wildman, K. A. H., Ramamoorthy, A. & Veglia, G. NMR structure of the cathelicidin-derived human antimicrobial peptide LL-37 in Dodecylphosphocholine micelles. *Biochemistry* **47**, 5565–5572 (2008).
12. Wang, G. Structures of human host defense cathelicidin LL-37 and its smallest antimicrobial peptide KR-12 in lipid micelles. *J. Biol. Chem.* **283**, 32637–32643 (2008).
13. Ramamoorthy, A., Lee, D.-K., Santos, J. S. & Wildman, K. A. H. Nitrogen-14 solid-state NMR spectroscopy of aligned phospholipid bilayers to probe peptide-lipid interaction and oligomerization of membrane associated peptides. *J. Am. Chem. Soc.* **130**, 11023–11029 (2008).
14. Wildman, K. A. H., Lee, D.-K. & Ramamoorthy, A. Mechanism of lipid bilayer disruption by the human antimicrobial peptide, LL-37. *Biochemistry* **42**, 6545–6558 (2003).
15. Chen, Z., Shen, Y. R. & Somorjai, G. A. Studies of polymer surfaces by sum frequency generation vibrational spectroscopy. *Annu. Rev. Phys. Chem.* **53**, 437–465 (2002).
16. Mermut, O., Phillips, D. C., York, R. L., McCrea, K. R., Ward, R. S. & Somorjai, G. A. In situ adsorption studies of a 14-amino acid leucine-lysine peptide onto hydrophobic polystyrene and hydrophilic silica surfaces using quartz crystal microbalance, atomic force microscopy, and sum frequency generation vibrational spectroscopy. *J. Am. Chem. Soc.* **128**, 3598–3607 (2006).
17. Guyot-Sionnest, P., Hunt, J. & Shen, Y. Sum-frequency vibrational spectroscopy of a Langmuir film: Study of molecular orientation of a two-dimensional system. *Phys. Rev. Lett.* **59**, 1597–1600 (1987).
18. Baker, L. R. *et al.* Furfuraldehyde hydrogenation on titanium oxide-supported platinum nanoparticles studied by sum frequency generation vibrational spectroscopy: acid-base catalysis explains the molecular origin of strong metal-support interactions. *J. Am. Chem. Soc.* **134**, 14208–14216 (2012).
19. Ye, H. K., Abu-Akeel, A., Huang, J., Katz, H. E. & Gracias, D. H. Probing organic field effect transistors in situ during operation using SFG. *J. Am. Chem. Soc.* **128**, 6528–6529 (2006).
20. Yang, Z., Li, Q. F. & Chou, K. C. Structures of Water Molecules at the Interfaces of Aqueous Salt Solutions and Silica: Cation Effects. *J. Phys. Chem. C.* **113**, 8201–8205 (2009).
21. Perry, A., Neipert, C. & Space, B. Theoretical modeling of interface specific vibrational spectroscopy: methods and applications to aqueous interfaces. *Chem. Rev.* **106**, 1234–1258 (2006).
22. Moore, F. G. & Richmond, G. L. Integration or segregation: how do molecules behave at oil/water interfaces? *Accounts. Chem. Res.* **41**, 739–748 (2008).
23. Weidner, T., Breen, N. F., Li, K., Drobny, G. P. & Castner, D. G. Sum frequency generation and solid-state NMR study of the structure, orientation, and dynamics of polystyrene-adsorbed peptides. *P. Natl. Acad. Sci. USA.* **107**, 13288–13293 (2010).
24. Jung, S.-Y. *et al.* Detecting protein-ligand binding on supported bilayers by local pH modulation. *J. Am. Chem. Soc.* **125**, 12782–12786 (2003).
25. Chen, X. *et al.* Specific Anion Effects on Water Structure Adjacent to Protein Monolayers. *Langmuir* **26**, 16447–16454 (2010).
26. Liu, J. & Conboy, J. C. Direct measurement of the transbilayer movement of phospholipids by sum-frequency vibrational spectroscopy. *J. Am. Chem. Soc.* **126**, 8376–8377 (2004).
27. Ma, G., Chen, X. & Allen, H. C. Dangling OD confined in a Langmuir monolayer. *J. Am. Chem. Soc.* **129**, 14053–14057 (2007).
28. vandenAkker, C. C., Engel, M. F. M., Velikov, K. P., Bonn, M. & Koenderink, G. H. Morphology and persistence length of amyloid fibrils are correlated to peptide molecular structure. *J. Am. Chem. Soc.* **133**, 18030–18033 (2012).
29. Chen, X., Wang, J., Sniadecki, J. J., Even, M. A. & Chen, Z. Probing α-Helical and β-Sheet Structures of Peptides at Solid/Liquid Interfaces with SFG. *Langmuir* **21**, 2662–2664 (2005).
30. Fu, L., Liu, J. & Yan, E. C. Y. Chiral sum frequency generation spectroscopy for characterizing protein secondary structures at interfaces. *J. Am. Chem. Soc.* **133**, 8094–8097 (2011).
31. Fu, L., Ma, G. & Yan, E. C. Y. In situ misfolding of human islet amyloid polypeptide at interfaces probed by vibrational sum frequency generation. *J. Am. Chem. Soc.* **132**, 5405–5412 (2010).
32. Nguyen, K. T., Soong, R., Lm, S.-C., Waskell, L., Ramamoorthy, A. & Chen, Z. Probing the spontaneous membrane insertion of a tail-anchored membrane protein by sum frequency generation spectroscopy. *J. Am. Chem. Soc.* **132**. 15112–15115 (2010).
33. Nguyen, K. T., Clair, S. V. Le., Ye, S. & Chen, Z. Molecular interactions between magainin 2 and model membranes in situ. *J. Phys. Chem. B.* **113**, 12358–12363 (2009).
34. Chen, X., Wang, J., Boughton, A. P., Kristalyn, C. B. & Chen, Z. Multiple orientation of melittin inside a single lipid bilayer determined by combined vibrational spectroscopic studies. *J. Am. Chem. Soc.* **129**, 1420–1427 (2007).
35. Moad, A. J. *et al.* NLOPredict: Visualization and Data Analysis Software for Nonlinear Optics. *J. Comput. Chem.* **28.** 1996–2002 (2007).

36. Ramamoorthy, A., Lee, D. K., Narasimhaswamy, T., & Nanga, R. P. Cholesterol reduces pardaxin's dynamics-a barrel-stave mechanism of membrane disruption investigated by solid-state NMR. *BBA-Biomembranes* **1798**, 223–227 (2010).
37. Wildman, K. A. H., Martinez, G. V., Brown, M. F. & Ramamoorthy, A. Perturbation of the hydrophobic core of lipid bilayers by the human antimicrobial peptide LL-37. *Biochemistry* **43**, 8459–8469 (2004).
38. Oren, Z., Lerman, J. C., Gudmundsson, G. H., Agerberth, B. & Shai, Y. Structure and organization of the human antimicrobial peptide LL-37 in phospholipid membranes: relevance to the molecular basis for its non-cell-selective activity. *Biochem. J.* **341**, 501–513 (1999).

Acknowledgements

This work was supported by the National Institute of Health (R01GM081655 to Z.C and A.R.). B. D. acknowledges the Barbour Scholarship from the University of Michigan. We thank Dr. Xiaofeng Han and Dr. Pei Yang for technical support. Insightful discussions with Lujie Huang and Dr. Andrew Boughton on orientation analysis, and Dr. Sathiah Thennarasu and Dr. Dong-Kuk Lee on the mechanism of action of LL-37 are also acknowledged.

Author contributions

Z.C., A.R. and B.D. designed the project, analyzed the data and wrote the manuscript. B.D. performed SFG experiments and developed the data analysis methods. L.S. prepared the cholesterol-related bilayer and participated in cholesterol-related SFG experiments. K.N. did some initial SFG experiments on LL-37. J.G. and X.Y. designed SPR experiments and collected SPR data.

Additional information

Supplementary information accompanies this paper at http://www.nature.com/scientificreports

Competing financial interests: The authors declare no competing financial interests.

How to cite this article: Ding, B. *et al.* Physiologically-Relevant Modes of Membrane Interactions by the Human Antimicrobial Peptide, LL-37, Revealed by SFG Experiments. *Sci. Rep.* **3**, 1854; DOI:10.1038/srep01854 (2013).